FROZEN SIZE PDF RESULTING FROM THE BREAK UP OF AN AIR BUBBLE INJECTED INTO A FULLY DEVELOPED TURBULENT FLOW

C. Martínez-Bazán
Departamento de Ingeníeria Mecánica, Universidad Carlos III
C/ Butarque 15, 28911 Leganés, Spain

J.L. Montañes
Departamento de Motopropulsión y Termofluidodinámica, ETSI Aeronáuticos (UPM)
Pz. Cardenal Cisneros 3, 28040 Madrid, Spain

J.C. Lasheras
Department of Applied Mechanics in Engineering Sciences
University of california, San Diego
9500 Gilman Drive, La Jolla, CA, 92093-0411, USA

ABSTRACT

The *frozen* bubble size distribution, resulting from the break up of an air bubble injected into a fully developed region of a high Reynolds number turbulent jet has been measured using a Phase Doppler Particle Analyzer (PDPA). It is shown that the shape of the distribution depends on ϵ and on initial void fraction, α. However, when the bubble's diameter is nondimensionalized with the Sauter Mean Diameter, D_{32}, of the distribution, the data is shown to collapse onto a single distribution, independent of ϵ and α.

INTRODUCTION

The droplet size distribution function resulting from turbulent break up has been largely studied since the initial work of Kolmogorov (1941). Statistical approaches have been used to obtain the probability distribution of droplet sizes in turbulent break-up processes (Cohen,1991), (Longuet-Higgings, 1992), (Brown and Wohletz, 1995) and (Novikov and Dommermuth, 1997) among others.

The objective of this work is to obtain detailed experimental measurements of the probability density function of the droplet sizes resulting from the break-up of an immiscible fluid injected into a turbulent flow of known characteristics. In order to isolate the problem, and to prevent the additional complexity introduced by the use of solid surfaces or any other moving surfaces to generate the turbulence, we selected to study the turbulent break-up by injecting air bubbles into the fully developed turbulent region along the central axis of a high Reynolds number water jet (the experimental facility has been described in detail elsewhere, Martínez-Bazán et al., 1999a). Through the use of Phase Doppler Techniques (PDPA) and image processing, we measured the transient *pdf* as well as the frozen *pdf* of the bubbles sizes resulting from the turbulent break-up over a wide range of initial bubble sizes and turbulent conditions characterized by the Turbulent Kinetic Energy (or the dissipation rate, ϵ) of the underlying turbulence. The measurements of the transient bubble size *pdf* were then used to evaluate the various elements comprising the existing break-up models such as the break frequency $g(D_o)$ (Martínez-Bazán et al., 1999a) and *daughter* droplets *pdf* $f(D, D_o)$ (Martínez-Bazán et al., 1999b) occurring from the break-up of a *mother* bubble of size D_o. The purpose of this paper is then to provide the fundamental knowledge of the characteristic properties of the *frozen* bubble size *pdf* achieved once the break-up process has concluded and its dependence on the fluid's properties (surface tension, viscosity and density ratio between the two fluids), flow properties (ϵ), and initial concentration of the bubbles in the flow (void fraction, α).The experimental measurements of the *frozen* bubble *pdf* are used to compared with the results obtained using the models for the break-up frequency and for the *daughter* bubbles *pdf* described in Martínez-Bazán et al. (1999a) and (1999b).

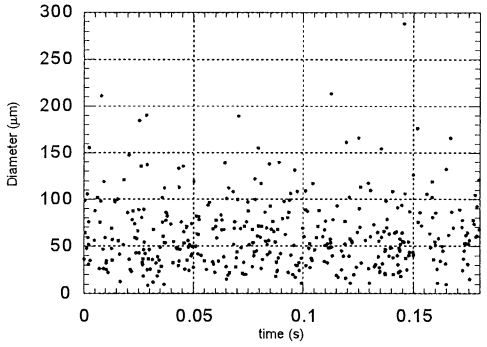

Figure 1: Time record of bubbles generated by a water jet. R_e=53,000.

INTER-ARRIVAL TIME BETWEEN BUBBLES

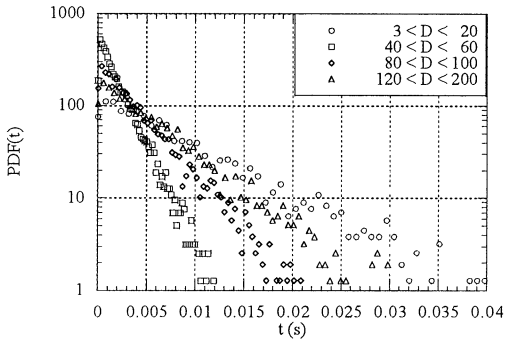

Figure 2: Inter-arrival time *pdfs* of different classes of bubbles. R_e=53,000.

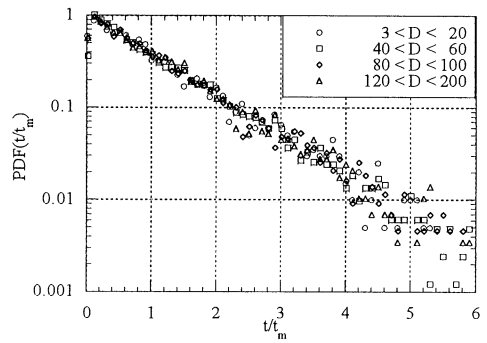

Figure 3: *Pdfs* of the normalized Inter-arrival time, t/t_m (t_m= mean inter-arrival time) of different classes of bubbles. R_e=53,000.

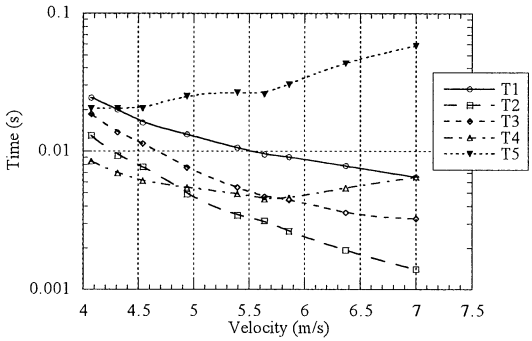

Figure 4: Evolution of Mean Inter-arrival time with the local convective velocity, U. The Reynolds Number of the jet has been varied from 32,000 to 60,000.

In addition to study the characterization of the break-up process and the time-averaged bubble size *pdf* described in the introduction, we have also analyzed the time series of the bubbles measured by the PDPA. Since we are able to measure not only the size of the bubbles crossing throughout the probe volume but also their velocity and the arrival time, we can compute the time and, consequently, the distance separating two consecutive bubbles of the same size. Therefore we can analyze the fluctuations of the concentration of bubbles and its dependence on the bubble size, D, dissipation rate of TKE, ϵ, and initial void fraction, α. Figure 1 shows a plot of a time series data of the bubble size diameter. It looks as if could be some clustering of occurrence times of the bubbles. This information can be very useful in order to study clustering events of bubbles of different sizes or infer the formation frequencies of bubbles if they are responding to certain frequencies of the flow. It is expected that bubbles of similar diameter will behave similarly in terms of formation and dispersion throughout the spray. If the bubble's Stokes number, defined as

$$St = \frac{D^2\, u'}{36\,\nu\,\delta}, \qquad (1)$$

where D is the diameter of the bubble, u' and δ are the characteristic velocity and length scales, and ν is the kinematic viscosity, is small in the range of bubble size of interest here, the effect of any clustering in the time series will be only the consequence of the break-up process.

The possible clustering shown in figure 1 by the concentration of a large number of bubbles within some intervals of time may indicate the presence of some kind of time correlation or it may be just the consequence of a random occurrence. In the analysis of the bubble-size probability density functions, the time dependence of the process is missing. Here we want to present some experimental measurements of the time series to establish if the break-up of bubbles by a turbulent flow contains some sort of time-correlated behavior.

In order to look for any possible time correlation in the break-up of bubbles, we should subdivide the bubble sizes in classes which might behave equally. For this purpose, the size distribution was divided in five size-bins, $3\,\mu$m $<$ D $<$ $20\,\mu$m, $40\,\mu$m $<$ D $<$ $60\,\mu$m, $80\,\mu$m $<$ D $<$ $100\,\mu$m, $120\,\mu$m $<$ D $<$ $200\,\mu$m, and $200\,\mu$m $>$ D. The time separating the arrival of two consecutive bubbles which belong to the same class was recorded. This provided information on the temporal variation of concentration of bubbles of different sizes as explained above. The probability density functions of the inter-arrival time corresponding to four of the size bins are given in figure 2 for the case of Re=53,000 and fixed flow rate of air. The distribution corresponding to the fifth size-bin, $200\,\mu$m $>$ D, is not represented due to the very small number of bubbles collected in this particular bin. The inter-arrival time *pdfs* have been plotted in a log-linear scale to highlight the fact that they are exponentially distributed. Notice that for the four size-bins presented, the probability of the inter-arrival time between two consecutive bubbles increases as the inter-arrival time decreases. There is not a predominant frequency (or time) at which bubbles are produced. Therefore the inter-arrival time *pdfs* do not show a high concentration of bubbles at that characteristic frequency. Imagine, for example, a flow in which bubbles of size D_1 are formed at a fixed frequency of 100 Hz. If we calculated the *pdf* of the time between two consecutive bubbles of size D_1 we would find a strong peak in the distribution for a value of t equal to 10 ms. Although the data presented in figure 2 correspond to an intermediate R_e = 53,000, it can be clearly seen that the *pdfs* follow exponential distributions of differ-

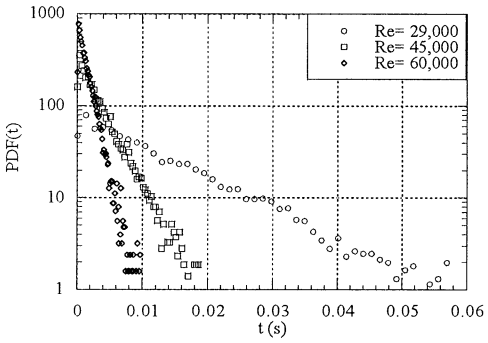

Figure 5: Evolution of the Inter-arrival time *pdf* of bubbles of size 40 μm < D < 60 μm with the Reynolds Number.

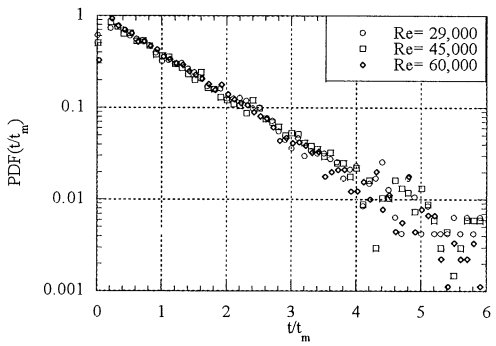

Figure 6: Evolution of the normalized Inter-arrival time *pdf* of bubbles of size 40 μm < D < 60 μm with the Reynolds Number.

ent mean value, $t_m = 1/\lambda$. An exponential distribution is given by the following equation,

$$PDF(t) = \lambda\, e^{-\lambda\, t}\ , \qquad (2)$$

where $t_m = 1/\lambda$ is the mean as well as the root-mean-square value of the distribution. The slopes of the tails represent the mean rate of arrival of bubbles of each size class. Note that we are able to represent with a unique distribution the *pdf* of the dimensionless time $t^* = t/t_m = \lambda\, t$,

$$PDF(t^*) = \ e^{-t^*}\ . \qquad (3)$$

The probability density functions of the inter-arrival time, normalized by the mean value, $t^* = t/t_m = \lambda\ t$, for the above cases has been represented in figure 3. As indicated by equation 3, when using the non-dimensional variable, t^*, the $pdfs(t^*)$ follow the same exponential distribution with slope -1. Since the exponential distribution provides the probability for the time between successive events occurring in a Poisson process, as one would expect, it appears that the process of formation on bubbles by a high intensity homogeneous turbulence is a random process which can be well represented by a Poisson distribution. This result would indicate that individual bubbles within the turbulent jet act independently of each other and, therefore, the movement of one of them is not conditioned by the neighboring ones. In a more dense case, where the particle's movement may influence the others, the exponential approximation may not apply.

Effect of the Turbulent Kinetic Energy on the inter-arrival time.

The time between two consecutive particles which belong to the same size-bin can be defined as:

$$\triangle t_i = \frac{1}{C_i\, U_i\, A}\ , \qquad (4)$$

where C_i = number of particles / Volume and U_i are the concentration and velocity of a bubble sized in class i, and A is the jet cross-section. Therefore, the inter-arrival time, $\triangle t_i$, increases as the concentration, C_i, and the velocity, U_i, decreases.

Figure 4 shows the evolution of the mean inter-arrival time of the five bubble size-bins defined above for various flow conditions. As the value of the mean velocity of the jet, U, becomes larger, the Reynolds number of the jet increases and consequently so does the value of the dissipation rate of turbulent kinetic energy, ϵ. Therefore, in addition to increasing the velocity of the bubbles, U_i, the number of bubbles may increase as well due to the break-up since the turbulent kinetic energy of the flow is larger. This is true for bubbles of small size which belong to class 1, (o), class 2, (□), and class 3, (◇), while large bubbles within class 5, (▼), increase their inter-arrival time since, although their velocity increases, this type of bubbles are broken as ϵ is increased. Bubbles of size class 4, (△), lessen their inter-arrival time until a point where the break-up effect is dominant and it starts increasing due to fact that the number bubbles of this class diminishes. The behavior of the standard deviation of the inter-arrival time is identical to that of the mean value. In fact, it has been found that the ratio of the rms to the mean value, t'/t_m, is unity in all cases as it would be expected if the inter-arrival *pdfs* were in fact exponential distributions.

To study the variation of the inter-arrival time with respect to the Reynolds number of the water jet, or similarly with respect to ϵ, which is the same in this case since the R_e is varied by changing the velocity at the exit of the nozzle, we have plotted in figure 5 the *pdfs* of the inter-arrival time of bubbles of size class 2, 40 μm < D < 60 μm, at three different values of the Reynolds number. The results are consistent with those shown in figure 4. As R_e is increased, the inter-arrival time of the class 2 bubbles decreases since their convective velocity is faster and more and more bubbles are produced due to the break-up of larger ones. Selecting a non-dimensional variable of time, t/t_m (t_m is the inter-arrival mean value), the probability density function, $pdf(t/t_m)$, has a self-similar behavior that can be perfectly represented by an exponential distribution, $pdf(t/t_m) = exp[-t/t_m]$, as shown in figure 6. The self-similar behavior is independent of the Reynolds number and of the diameter of the bubble, and the possible clustering (if any) mentioned in the beginning is, therefore, the product of a random process.

INTER-ARRIVAL DISTANCE BETWEEN BUBBLES

The properties of the time between two consecutive bubbles, explained in the previous section, are very interesting. Another important aspect of the process is the knowledge of the concentration of bubbles, in other words, the knowledge of the distance between two consecutive bubbles which belong to the same bubble size-class. The distance between two consecutive bubbles of the same class is calculated from their corresponding inter-arrival time, $\triangle t_i$, and their convective velocity, U_i, as:

$$\triangle l_i = \triangle (t_i U_i) = \frac{1}{C_i A} . \qquad (5)$$

The probability density function of the distance between two consecutive bubbles of the same size follow the same characteristics as those mentioned for the inter-arrival time. As would be expected, since bubbles of the same size move at the same velocity, the *pdf* of the inter-arrival distance of bubbles within the same class follows an exponential distribution with an intensity parameter, λ, which only depends on the number (concentration) of particles of a certain class "*i*", C_i. Figure 2, in the previous section, shows that the steepest slope of the inter-arrival time *pdfs* corresponds to the bubble-size class 2 ($40\,\mu m < D < 60\,\mu m$), followed by bubble-size class 3 ($80\,\mu m < D < 100\,\mu m$), bubble size-class 4 ($120\,\mu m < D < 200\,\mu m$) and, finally, the least steep one corresponds to bubble-size class 1 ($3\,\mu m < D < 20\,\mu m$). The same trend is appreciable for the *pdfs* of the inter-arrival distance (not shown due to space limitations in this paper), $\triangle l_i = \triangle (t_i U_i)$, indicating that the convective velocities of all bubble-size classes, U_i, are the same and equal to that of the mean flow.

From the above results on the inter-arrival time an inter-arrival distance, we observe that the bubbles are not formed in a predictable fashion but, instead, they are created and dispersed in a random way. Edwards and Marx (1995a) developed a theoretical framework for the analysis of the time-based statistics of sprays. Based on their approach, the measured bubbly jet behaves as an *ideal spray* driven by many superposed Poisson processes (of bubble sizes), each one characterized by a continuous intensity function. Therefore, and establishing an analogy with the properties of an *ideal spray* (Edwards and Marx, 1995b), the characteristics of the family of bubbles formed by the break-up of a volume of air introduced into a turbulent water flow are the following:

- The bubbles are modeled as non-interacting particles. The effect of bubbles collision is negligible. Individual behavior of different bubble-size classes is independent on each other.
- Each of the particles carries a set of marks that represent the characteristic of the bubble being considered, i.e., velocity, size, etc.
- The bubble field is not highly ordered. Therefore it is in some sense random.
- The statistics of the bubble field are not affected by events in the past or in the future, only by the present. This means that the probability of finding a bubble at a certain location at a fixed time is only a function of the location and the time and not whether others bubbles exist nearby.

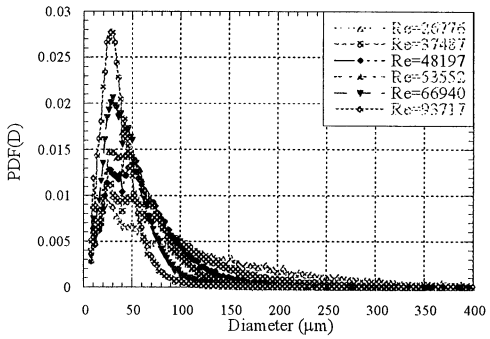

Figure 7: Frozen bubble size *pdf* for various Reynolds numbers of the submerged water jet.

All bubbles, produced by the break-up of an air mass injected into a turbulent water jet, are created and transported downstream in the same way. The *pdfs* of the inter-arrival time or distance between two consecutive bubbles of the same class follow the exponential distribution, characteristic of steady state case, developed by Edwards and Marx (1995b). Therefore, all bubbles, in the range of bubble size and jet Reynolds numbers presented here, feel the influence of the water jet which, at its axis, can be characterized as isotropic and homogeneous turbulent flow. Measurements at the edge of the water jet would indicate a preferential concentration of those bubbles transported by large scales. These results would be shown in the above *pdfs* as a strong deviation from their exponential distribution. Similar type of measurements have been presented by Edwards and Marx (1995b), for very small particles, which follow the flow, measured in the internal shear layer of a kerosene spray flame.

DEPENDENCE OF THE FROZEN BUBBLE SIZE *PDF* ON ϵ

The measured frozen bubble size *pdfs* are shown in figure 7. These measurements were obtained by fixing the injection flow rate of the air while systematically increasing the Reynolds number of the water jet. Each one corresponds to a given jet Reynolds number, which in turn represents a certain value of ϵ at the injection point. For convenience, since the diameter of the water nozzle, D_J, and the air injection point, $X/D_J = 10$, have been kept constant, the Reynolds number of the submerged jet, $R_e = \frac{U_0 D_J}{\nu}$, will be used as a parameter to indicate increasing levels of turbulent kinetic energy existing at the bubble's injection point. The first important conclusion, evident from these results, is that the shape of the bubble size *pdf* strongly depends on the turbulent kinetic energy (or dissipation rate ϵ) of the underlying turbulence. As the value of ϵ at the air injection point increases, the lump of air injected into the turbulent jet is subjected to stronger turbulent stresses. Consequently the value of the critical bubble's diameter, D_c, decreases. This result is apparent in figure 7 where it is seen that as the Reynolds number is increased the *pdf* becomes narrower, indicating that the large bubbles have been broken, generating, a large number of small ones.

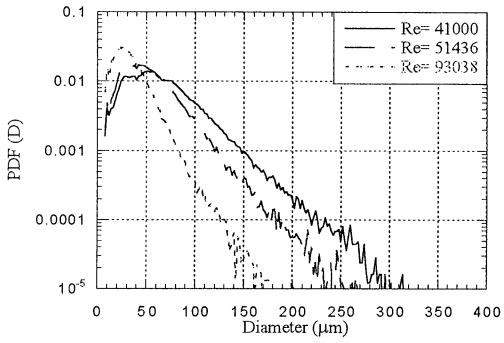

Figure 8: Evolution of the bubbles size *pdf* with the Reynolds number. $Q_a = 3.6$ ml/min.

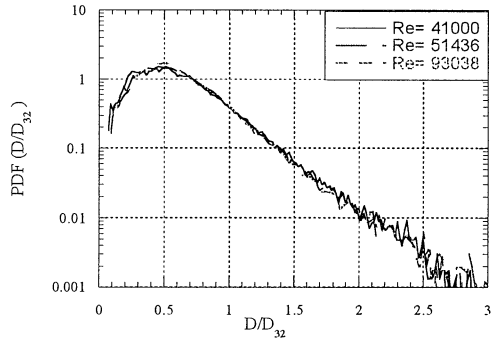

Figure 9: Bubble size *pdf* of $\hat{D} = D/D_{32}$. $Q_a = 3.6\, ml/min$.

To study the evolution of the shape of the bubble size *pdf* with the turbulent stresses acting on the surface of the bubbles, we conducted a series of experiments where ϵ was varied while keeping constant the flow rate of air injected into the flow. The water jet Reynolds number was increased from $R_e = 28,000$ to $R_e = 93,000$ for three different values of the flow rate of air, $Q_a = 3.6$ ml/min, $Q_a = 7.25$ ml/min, and $Q_a = 34.35$ ml/min. The experimental measurements corresponding to the lowest flow rate of air are presented in figure 8 where for simplicity we have represented the bubble size *pdf* for only three values of the R_e. The slope of the exponential tails of the *pdfs* increases with the R_e, a consequence of the decrease of the largest bubble size with R_e. In order to represent the bubble size *pdf* in non-dimensional variables, we chose D_{32} as the normalization bubble's diameter and we defined $\hat{D} = D/D_{32}$. The probability density function of $\hat{D}$, $pdf(\hat{D})$, for the same experiments previously shown in figure 8 are given in figure 9. It is very important to remark that all the $pdfs(\hat{D})$ collapse on a single curve, showing that the slope of the tails of the bubbles size distribution is just a function of the maximum bubble's diameter, characterized in these cases by D_{32}. The same type of behavior, although not shown here, has been observed for the other cases tested at $Q_a = 7.25$ ml/min, and $Q_a = 34.35$ ml/min.

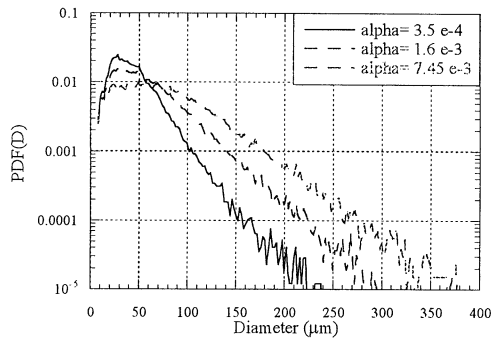

Figure 10: Evolution of the bubbles size *pdf* with the air void fraction, α. $R_e = 54036$.

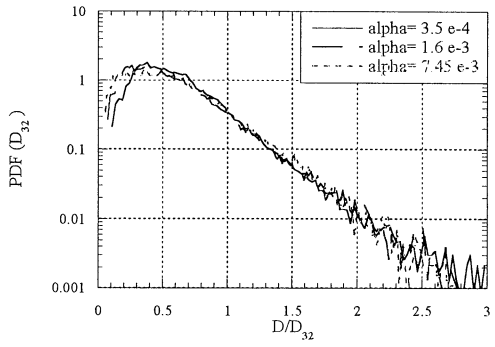

Figure 11: Bubble size *pdf* of $\hat{D} = D/D_{32}$. $R_e = 54036$.

DEPENDENCE OF THE FROZEN BUBBLE *PDF* ON THE INITIAL VOID FRACTION, α

The effect of the initial air void fraction, $\alpha = Q_a/Q_w$, on the shape of the frozen *pdf* is shown in figure 10. These *pdfs* correspond to a representative intermediate jet Reynolds number of $R_e = 54,036$, varying the void fraction by nearly two orders of magnitude. Qualitatively, the observed effect of increasing the void fraction appears to be very similar to the effect of decreasing the value of the dissipation rate. The slope of the tails of the *pdfs* increase as α decreases. Although the effect of α on the shape of the *pdfs* is noticeable, it is not as strong as the effect of ϵ discussed earlier. As was the case in the evolution of *pdf* with ϵ, the $pdfs(\hat{D})$, where $\hat{D} = D/D_{32}$, also collapse in a single, self-similar curve showing that D_{32} is the only parameter needed to describe the behavior of the frozen bubble's size *pdf*, see figure 11.

The possible causes of the changes in the *pdfs* with α are coalescence, modifications in the turbulent energy spectra due to the presence of the bubbles which translate into lower values of the ϵ, increasing therefore the value of the critical diameter, $D_c \propto (\sigma/\rho)^{3/5}\, \epsilon^{-2/5}$, and consequently the value of D_{max}, or a combination of both effects. To account for the effect due to changes in ϵ the energy spectrum was measured using hot film anemometry, at a point downstream in the jet where the break-up takes place, radially displaced a distance close to the jet's centerline but far enough to avoid any

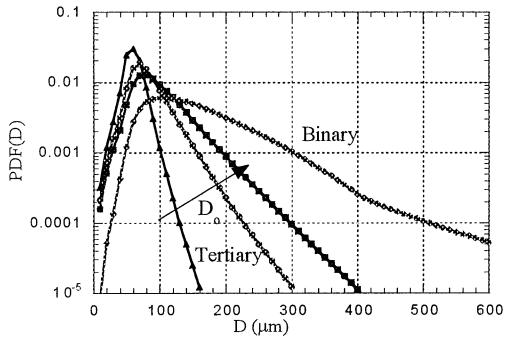

Figure 12: Evolution of pdf(D) with the size of the initial lump of air, D_o.

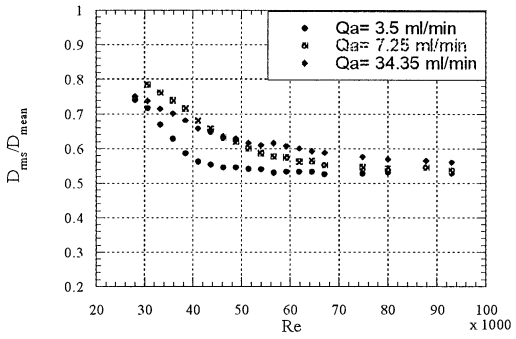

Figure 13: Evolution of D_{rms}/D_{mean} with the water jet Reynolds number at various values of Q_a.

contact of the bubbles with the probe. Therefore, if the energy spectrum was affected by the bubbles, an indirect effect at the measuring point would have been detected. We are more inclined to think that the changes in the $pdf(D)$ with initial air void fraction are a consequence of the memory of the initial conditions. As the initial void fraction, α, increases, the initial lump of air immersed into the flow is larger and consequently its break-up frequency is smaller as shown by Martínez et al. (1999a). Since the dissipation rate of turbulent kinetic energy, ϵ, decreases in a jet with the downstream distance, the bubbles encounter regions of lower ϵ as they are transported by the mean motion of the flow. Therefore, the measured *pdf* is a frozen one which did not have time to reach an equilibrium during the residence time of the bubbles within regions of nearly constant ϵ. This effect is shown in figure 12 where we have presented the frozen $pdf(D)$ obtained with our break-up model, described in Martínez et al. (1999b), for three different initial bubble's diameter. Notice the similarity between figure 10 mesured experimentally and figure 12 obatined with our mode. As the size of the initial lump of air,D_o, increases, the frozen $pdf(D)$ becomes wider producing, therefore, larger bubbles. An important issue to be considered in the model is the question of binary or tertiary break-up. Figure 12 shows that a model based on a binary break-up process will result in a much wider frozen $pdf(D)$.

Experimental evidence of the frozen $pdf(D)$ is shown in figure 13 where we have plotted the evolution of the ratio of root-mean-square to the mean values of the measured distribution with the jet's Reynolds number at three different values of Q_a. The value of D_{rms}/D_{mean} decreases with R_e until it reaches a constant value of $\approx$ 0.54 which is independent of R_e and Q_a. These results show that at high R_e, at which the break time is shorter than the residence time, the obtained $pdf(D)$ has time evolve to the equilibrium one. On the other hand, at lower values of R_e, where the residence time is shorter that the break-up time, the measured $pdf(D)$ have been frozen due to the decrease of the local value of ϵ

CONCLUSION

We have studied the shape of the bubble size *pdf* resulting from the turbulent break up of a continuos air jet injected into a fully developed region of a turbulent, axisymmetric water jet. The frozen *pdfs* are shown to be strongly dependent on the dissipation rate of turbulent kinetic energy of the underlying turbulence, ϵ, and on the initial air void fraction, α. Furthermore, it has been found that when the bubble's diameter is made dimensionless with the Sauter Mean Diameter of the distribution, D_{32}, the *pdfs* collapse into a single, universal function, independent of ϵ and of α.

Acknowledgements : The authors gratefully acknowledge the support of the ONR under contract # N00014-96-1-0213 and also the support of a Fellowship from the Consejo Asesor the Investigación de la Diputación General de Aragón (Spain) to Carlos Martínez-Bazán.

REFERENCES

Cohen, R.D.,1991, "Shattering of a liquid drop due to impact," *Phil. Trans. R. Soc. London Ser. A,* 435:483-503.

Edwards, C.F., and Marx, K.D., 1995a, "Multipoint statistical structure of the ideal spray, part I: Fundamental concepts and the realization density," *Atomization and Sprays,* Vol.5:435-455.

Edwards, C.F., and Marx, K.D., 1995b, "Multipoint statistical structure of the ideal spray, part II: Evaluation of steadiness using the interparticle time distribution," *Atomization and Sprays,* Vol.5:457-505.

Kolmogorov, A.N., 1941, "Logaritmically normal distributions of fragmentary particles," *Dokl. Akad. Navk. SSSR,* 31:99-101.

Longuet-Higgins, M.S., 1992, "The crushing of air cavities in a liquid," *Phil. Trans. R. Soc. London Ser. A,* 439:611-626.

Martínez-Bazán, C., Montañes, J.L., and Lasheras, J.C., 1999a, "On the break-up frequency of an air bubble injected into a fully developed turbulent flow," *Journal of Fluid Mechanics.* Under consideration for publication.

Martínez-Bazán, C., Montañes, J.L., and Lasheras, J.C., 1999b, "On the size PDF resulting from the break up of an air bubble immersed into a turbulent liquid flow," *Journal of Fluid Mechanics.* Under consideration for publication.

Novikov E.A., and Dommermuth D.G., 1997, "Distribution of droplets in a turbulent spray," *Physical Review E,* 56, No. 5:5479-5482.